科学通报 2017 年 第 62 卷 第 36 期: 4237 ~ 4255
评 述
《中国科学》杂志社
SCIENCE CHINA PRESS

# 面向微电子应用的二维过渡金属硫族化合物制备进展

许浒, 廖付友, 郭仲勋, 郭晓娇, 周鹏, 包文中*, 张卫

复旦大学微电子学院, 专用集成电路和系统国家重点实验室, 上海 200433
* 联系人, E-mail: baowz@fudan.edu.cn

2017-08-03 收稿, 2017-09-24 修回, 2017-09-27 接受, 2017-11-10 网络版发表
国家重点研发计划(2016YFA0203900)和国家自然科学基金(61376093, 61622401)资助

**摘要** 二维原子晶体材料所独有的结构特性带来了诸多优异的性质. 与石墨烯相比, 二维过渡金属硫族化合物(TMDs)拥有不同大小且可调控的带隙, 在微电子和光电器件领域有着广阔的应用前景. 本文对二维TMDs材料"自上而下"和"自下而上"的制备方法进行了总结, 对比了机械剥离、液相剥离和化学气相沉积等常见制备技术, 并归纳了各自的优缺点. 同时基于未来晶圆级二维TMDs器件, 重点介绍了化学气相沉积法及其面向应用需要解决的问题. 最后总结了二维TMDs材料在微电子器件应用中的研究进展.

**关键词** 二维层状材料/二维原子晶体, 过渡金属硫族化合物, 二硫化钼, 化学气相沉积

自石墨烯首次被发现以来[1~3], 二维原子晶体因其特殊的层状结构和丰富的物理化学性质引起了广泛关注. 这一类材料层内的原子是以强离子键或者共价键连接, 而层与层之间是以弱的范德华力堆叠在一起. 因此二维原子晶体很容易通过微机械剥离和离子插层的方法获得单层的材料[2]. 近十年的时间里, 石墨烯因其出众的电学、光学和化学性质而备受人们青睐, 但是由于石墨烯天然的零带隙, 往往需要复杂的手段才能打开一定的带隙, 这就限制了石墨烯在电子与光电子方向的应用[4,5], 从而激励了研究者继续探索新的二维材料. 以$MoS_2$, $WSe_2$等过渡金属硫族化物(transition metal dichalcogenides, TMDs)为代表的一系列类石墨烯二维(2D)层状材料, 因其可调控的禁带宽度引起了人们的注意. TMDs材料都是由$MX_2$结构组成, 其中M为过渡金属元素(比如Mo, W, Ti, Pt, Re, Ta等), X是硫族元素(比如S, Se, Te)[6,7]. 由于众多的元素组合, 二维TMDs显示了丰富的电学性质, 从半导体到半金属, 甚至是超导体[8~10], 如表1所示[11]. 此外, 一些二维TMDs材料的禁带宽度还可以由层数、应力和堆叠方式来调控[12~16]. 这些特性都为将来的器件应用提供了更多的灵活度.

目前, 二维TMDs材料走向实际应用仍然有许多挑战需要克服. 首先, 现阶段对二维TMDs基础物理特性的探索尚在进行中, 如何有效调控这些特性并使之能够与实际器件应用需求相匹配, 仍需要进行大量的基础研究工作; 譬如对电子器件来说, 二维TMDs材料的载流子迁移率与石墨烯相比要低几个数量级, 从而限制了器件的驱动能力和工作速度[17~21]; 而对光电器件来说, 如何充分利用二维TMDs材料丰富的能带差异, 以及探索新型异质、复合材料的光电特性, 仍需要进行更深入的研究[11,22~27]; 最后, 二维TMDs真正能够实现应用的关键是材料的大面积可控制备及其器件工艺.

由于二维TMDs材料的能带结构与层数密切相关, 因此如何实现特定层数的可控制备尤为重要. 目前可以实现单层或者少层材料的制备技术可分为"自上而下"和"自下而上"两种. "自上而下"制备技术主要包括微机械剥离法[28]、离子插层剥离法[29]、液相

**引用格式**: 许浒, 廖付友, 郭仲勋, 等. 面向微电子应用的二维过渡金属硫族化合物制备进展. 科学通报, 2017, 62: 4237–4255
Xu H, Liao F Y, Guo Z X, et al. Recent progress in two-dimensional transition metal dichalcogenides: Material synthesis for microelectronics (in Chinese). Chin Sci Bull, 2017, 62: 4237–4255, doi: 10.1360/N972017-00851

**表 1 不同二维层状TMDs材料的电学特性**

**Table 1** Electronic properties of different 2D-TMDs

| 族序数 | 过渡金属元素M | 硫族元素X | 物理特性 |
|---|---|---|---|
| 4 | Ti, Hf, Zr | S, Se, Te | 半导体($E_g$=0.2~2 eV); 抗磁性 |
| 5 | V, Nb, Ta | S, Se, Te | 窄带金属($\rho$~$10^{-4}$ Ω cm)或半金属; 超导体; 顺、反铁磁性或抗磁性 |
| 6 | Mo, W | S, Se, Te | 硫化物和硒化物为半导体($E_g$~1 eV). 碲化物为半金属($\rho$~$10^{-3}$ Ω cm); 抗磁性 |
| 7 | Tc, Re | S, Se, Te | 小间隙半导体; 抗磁性 |
| 10 | Pd, Pt | S, Se, Te | 硫化物和硒化物为半导体($E_g$=0.4 eV), 抗磁性; 碲化物为金属, 顺磁性; $PdTe_2$为超导体 |

超声剥离法[30]等. 在“自下而上”制备技术中, 对化学气相沉积技术(chemical vapor deposition, CVD)[31,32]的研究已经展示了该方法在获得空间均一性良好、厚度可控的大面积薄膜的巨大潜力. 本文以两种制备方法为切入点, 对主流的二维TMDs制备技术的最新进展进行了归纳, 并介绍了其在电子器件应用中的前景.

## 1 二维TMDs的制备

根据制备二维TMDs薄片途径的不同, 一般可以将其制备方法分成两大类: 一类是通过TMDs的晶体块体剥离出二维TMDs薄片, 称之为“自上而下(top-down)”的方法; 另一类是在一定的实验条件下将对应的前驱体通过化学反应得到原子层厚度的TMDs晶体或者薄膜, 称之为“自下而上(down-top)”的方法.

### 1.1 “自上而下”的方法

“自上而下”的方法是在外界作用力下克服材料层间的范德华力, 使单层或者多层二维TMDs薄片从块体材料中剥离出来的方法. 这类方法的优点是原理简单, 操作方便. 常见的“自上而下”制备方法有微机械剥离法(micromechanical exfoliation)、离子插层剥离法(ion intercalation and exfoliation)、液相超声剥离法(liquid phase exfoliation by sonication), 此外也有激光热剥蚀(laser thinning technique)和热退火(thermal annealing)等方法的报道.

#### 1.1.1 微机械剥离法

微机械剥离法是通过外加机械力的方法从层状块体材料中分离出薄片的方法[29]. 该方法是一种制备二维层状材料薄片的传统方法, 早期就有利用胶带制备多层$MoS_2$[33]和利用原子力显微镜(AFM)或者扫面隧道显微镜(STM)针尖与石墨片的相互作用剥离出多层石墨烯的报道[34,35]. 2004年, 英国曼切斯特大学Geim和Novoselov采用微机械剥离的原理, 用胶带反复减薄石墨片得到了单层石墨烯[2], 接着又用同样的方法得到了单层的h-BN, $MoS_2$, $NbSe_2$和$Bi_2Sr_2CaCuO_x$等[29]. 近年来, 微机械剥离法被广泛用于制备单层石墨烯, h-BN, TMDs和其他类石墨烯的单层薄片[36~38]. 衬底类型的选择也有着重要影响. Si衬底上热氧化$SiO_2$(300 nm)的双层结构, 是现阶段用于二维层状材料的最常用衬底类型. 这种衬底能够增强对不同厚度二维原子晶体薄膜的光学干涉对比, 易于进行二维层状材料的层数判断; 同时由于掺杂Si良好的导电性, 也适合于制作成背栅(back-gated)场效应晶体管, 降低器件工艺难度.

利用微机械剥离法制备二维TMDs的一般过程如图1(a)~(f)所示, 首先利用常规的透明胶带(Scotch tape)或者无残留的低黏性胶带(Nitto)在块体材料上撕下1层很薄的材料, 然后将胶带反复对折黏揭, 当胶带上的材料减薄到一定程度后, 将胶带黏附在干净的$SiO_2$/Si衬底上, 撕下胶带后, 底上便会留下不同厚度的薄片, 在光学显微镜下根据薄片的颜色可以简单分辨出单层或多层的薄片, 如图1(g)~(j)所示, 在$SiO_2$(300 nm)衬底上用光学对比度、AFM和高分辨透射电子显微镜(HRTEM)等设备可以表征其厚度.

微机械剥离法工艺简单、成本较低, 得到的单层或多层二维TMDs薄片具有良好的晶体结构, 缺陷较少, 能够在空气中稳定保存较长时间, 适用于一些基本的表征和制作单个的器件. 相比于分子束外延(MBE)制备单层材料的方法, 微机械剥离法给科学研究提供了极大的便利. 目前已有诸多基于微机械剥离法制备的单层或多层二维TMDs薄片的研究报道, 例如低功耗电子器件[43]、光电器件[44]、自旋电子器件[45]、存储器[46]、传感器[47]和逻辑电路[48]以及谷电子学[49,50]、量子霍尔效应[51,52]、超导[53]和拓扑学[54]等. 但是该方法很难控制二维TMDs薄片的面积、厚

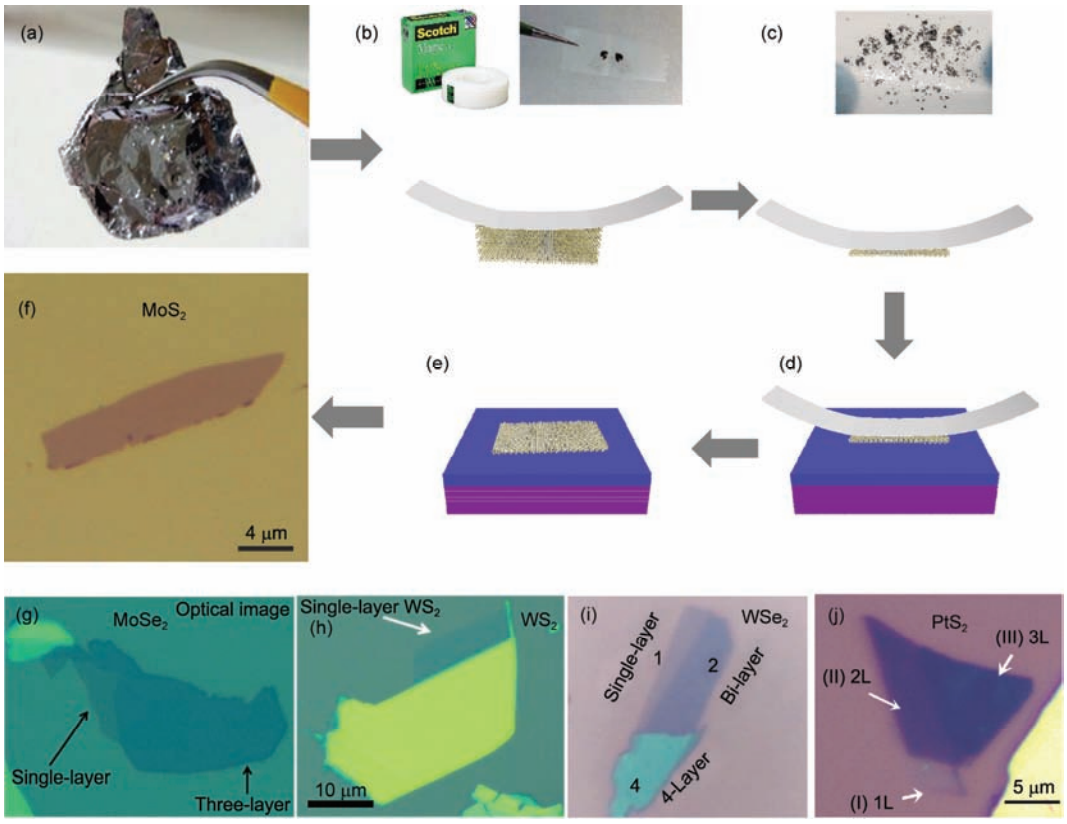


**图 1** (网络版彩色)微机械剥离法制备二维TMDs材料. (a) 微机械剥离法制备单层$MoS_2$的示意图[39]. 微机械剥离法制备的$MoSe_2$(b)[40], $WS_2$(c)[41], $WSe_2$(d)[41]和$PtS_2$(e)[42]薄片的光学显微镜照片

**Figure 1** (Color online) 2D TMDs materials prepared by the micromechanical exfoliation method. (a) The schematic of monolayer $MoS_2$ prepared by the micromechanical exfoliation method[39]. Optical microscope images of individual $MoSe_2$ (b)[40], $WS_2$ (c)[41], $WSe_2$ (d)[41] and $PtS_2$ (e)[42] sheets prepared by micromechanical exfoliation

度、形状, 并且重复性和产率较低.

### 1.1.2 锂离子插层剥离法

尽管微机械剥离法能够较容易在得到晶体结构近乎完美的原子级厚度2D TMDs, 但是该方法产率低、重复性差, 限制了其实际应用. 锂离子插层剥离法是可以在溶液中制备大量二维层状材料薄片的方法. 1975年, 最初由Dines[41]报道了锂离子插层法制备二维TMDs. 1986年, Joensen等人[55]对该方法加以改进, 并得到了单层$MoS_2$. 随着二维层状材料成为研究热潮, 锂离子插层法得到了进一步的发展和应用. 锂离子插层剥离法制备$MoS_2$薄片的步骤如图2(a)所示, 先将$MoS_2$块体制成粉末, 然后将$MoS_2$粉末和正丁基锂混合于正己烷溶液, 惰性气体环境下加热到100℃反应3 d, 得到剥离插层物; 加入一定量的去离子水, 接着超声1 h, 过滤、离心悬浊液并用去离子水多次洗涤至中性, 最后真空干燥即可得到$MoS_2$薄片, 如图2(c), (d)所示. 利用该方法可以得到大量亚微米尺寸的单层薄片[59], 但是这些单层材料的晶体结构和电学性能均发生了改变[30]. 例如离子插层法制备的单层$MoS_2$是金属相, 从2H-$MoS_2$变成了1T-$MoS_2$[30,60], 需要经过300℃退火后才能恢复半导体属性[30]. 锂离子插层法需要时间较长(超过1 d), 而且锂金属在空气中易燃, 通常需要在惰性气体的保护下进行, 同时锂的价格较贵, 这些缺点限制了其应用.

2011年, Zeng等人[58,61]发展了一种更快、更易控制的电化学离子插层剥离法, 用该方法制备得到石墨烯、h-BN和各种二维TMDs薄片. 其具体流程如图2(b)所示, 在一个锂离子电池装置中, 块体TMDs材料作为阴极, 锂箔作为阳极. 放电之后(锂离子插入层间), 把插层物(如$Li_xMoS_2$)放入水或乙醇中超声. 锂在水或乙醇中会产生氢气, 氢气把相邻的$MoS_2$层分离开, 最终得到分散充分的$MoS_2$薄片, 如图2(e), (f)所示. 普通的化学锂离子插层剥离法通常需要较

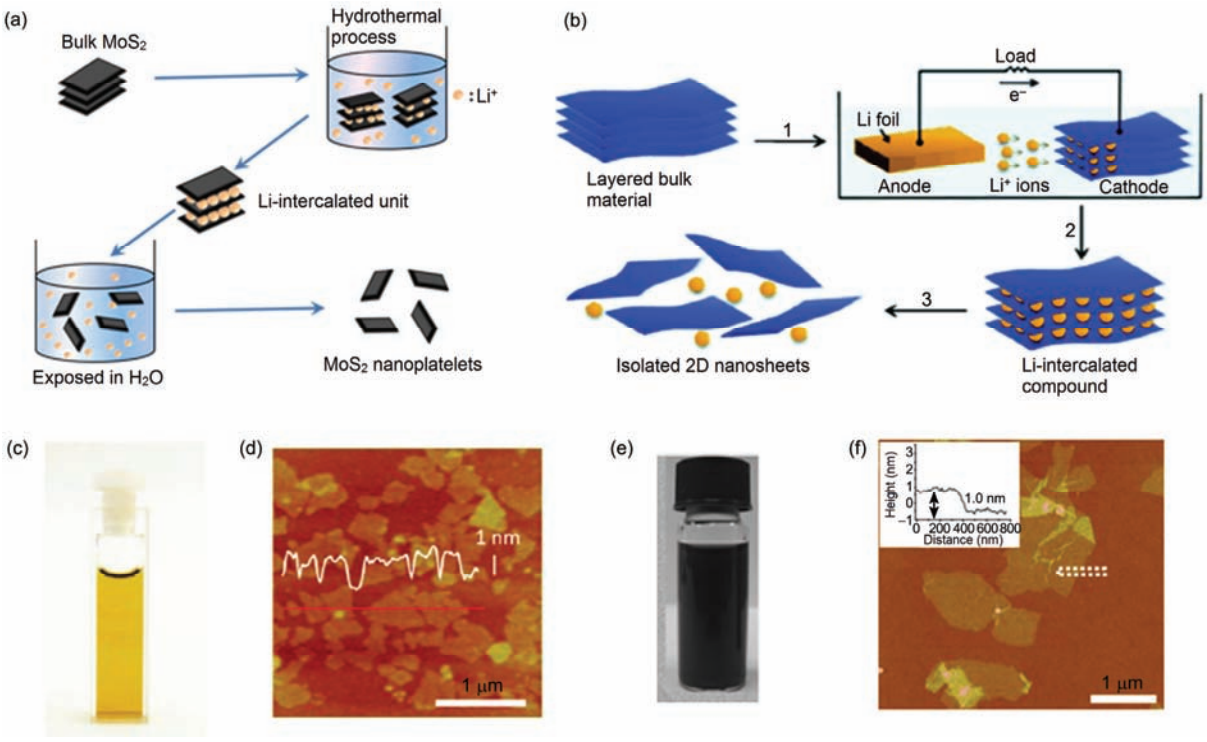


**图 2** (网络版彩色)锂离子插层剥离法制备二维TMDs材料. (a) 锂离子插层剥离法制备单层或多层$MoS_2$过程示意图[56]; (b) 电化学锂离子插层剥离法制备二维层状材料过程示意图[57]; 锂离子插层剥离法制备的$MoS_2$水溶液照片(c)和300℃退火后的单层$MoS_2$ AFM图(d)[30]; 电化学锂离子插层剥离法制备的$MoS_2$ NMP溶液照片(e)和$MoS_2$单层的AFM图(f)[58]

**Figure 2** (Color online) 2D TMDs materials prepared by lithium intercalation and exfoliation. (a) The schematic of preparing monolayer or multilayer $MoS_2$ sheets by lithium intercalation and exfoliation[56]. (b) The schematic of preparing 2D TMDs sheets by electrochemical lithium intercalation process[57]. Photograph of lithium intercalated $MoS_2$ suspension in water (c) and corresponding AFM image of exfoliated $MoS_2$ sheets after annealing at 300°C (d)[30]. Photograph of electrochemical intercalated $MoS_2$ suspension in NMP (e) and corresponding AFM image of individual $MoS_2$ sheet (f)[58]

高的温度和较长的反应时间[62], 而电化学离子插层剥离法在室温下只需要几个小时即可完成, 而且可以通过监测放电曲线来控制离子插入过程和数量, 大大地提高了效率. 但是其制备条件较严格, 且去除锂离子容易导致二维TMDs的聚集.

### 1.1.3 液相超声剥离法

液相超声法通常将二维层状材料的块体粉末分散到水或有机溶剂中, 通过超声波的能量将单层或多层薄片从其块体材料表面剥离, 如图3(a)所示. 液相超声剥离法也是大量制备二维TMDs薄片的候选方法之一, 该方法可以克服锂离子插层法操作不便及不安全的缺点. 一般来说, 液相超声剥离法制备的薄片尺寸有几百纳米, 剥离的薄片因为吸附了溶液中的分子相互排斥, 因而可以稳定存在, 不会团聚. 该方法最初用于制备石墨烯[65~67], 后来被用来制备各种二维TMDs[63,64,68,69]和其他二维层状材料薄片[71,72]. 2011年, Coleman研究组[69,70]采用液相剥离的方法制备了$MoS_2$, $WS_2$, $MoSe_2$, $NbSe_2$, $TaSe_2$, $NiSb_2$, $MoSb_2$, h-BN和BiSb薄片, 并尝试了多种普通溶剂来提高超声解离二维层状材料的剥离效率. 结果发现, 不同的二维层状材料适合的溶剂并不相同, 例如, 在*N*-甲基吡咯烷酮(NMP)溶液中超声剥离$MoS_2$, 可以较好地分散剥离下来的薄片; 水和乙醇的混合溶液也可以作为分散二维层状材料薄片的溶剂[64]. 通过混合不同种类的层状材料和分散体溶液, 也可以得到复合材料. 例如, $MoS_2$薄片混合石墨烯可以用作机械增强填料. 液相超声剥离法操作简单, 可以大规模生产, 但剥离程度和剥离效率一般不高, 得到的薄片溶液浓度较小, 产物中单层薄片的含量较低, 对超声条件依赖性高, 超声功率过大和过小都不利于薄片的形成.

### 1.1.4 激光热剥蚀和热退火

激光热剥蚀利用激光灼烧的方法将多层的二维层状材料减薄, 通过控制激光的波长和功率可以得

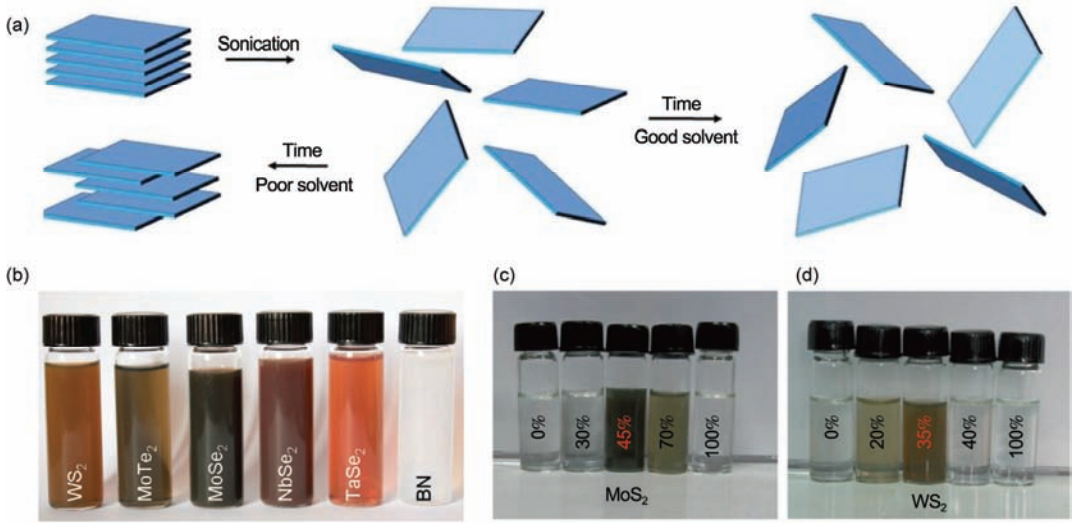


**图 3** (网络版彩色)液相超声法制备二维TMDs材料. (a) 液相超声法剥离二维TMDs示意图[30]; (b) 分别含有$WS_2$, $MoTe_2$, $MoSe_2$, $NbSe_2$, $TaSe_2$和h-BN薄片的水溶液照片[63]; $MoS_2$薄片(c)和$WS_2$薄片(d)分散在不同乙醇/水比例的混合溶液照片[64]

**Figure 3** (Color online) 2D TMDs materials prepared by liquid phase sonication. (a) Schematic description of liquid phase exfoliation by sonication to prepare 2D TMDs[30]. (b) Photograph of dispersions of $WS_2$, $MoTe_2$, $MoSe_2$, $NbSe_2$, $TaSe_2$, and BN stabilized in water by sodium cholate[63]. Photographs of $MoS_2$ (c) and $WS_2$ (d) dispersions in various ethanol-water mixtures, respectively[64]

到不同厚度的二维层状材料. 2011年, Han等人[73]采用激光辐照多层石墨烯制备了高质量的单层石墨烯. 2012年, Castellanos-Gomez等人[74]采用激光热剥蚀的方法得到了单层$MoS_2$, 如图4(a)~(c)所示, 其光学和电学性能与微机械剥离法得到的单层二硫化钼相似. 激光热剥蚀法在保证单层材料晶体质量的情况下, 可以控制二维层状材料薄片的厚度、面积和形状, 但是激光的成本昂贵, 因此激光热剥蚀的方法不能适用于大规模的工业生产.

热退火方法也可以将多层的二维层状材料薄片持续减薄至单层. 2013年, Lu等人[75]在650℃, 氩气压强为$1.33\times10^3$ Pa, 为5 sccm的石英管式炉中, 可以逐层地减薄多层$MoS_2$薄片, 如图4(d)~(k)所示, 速率约1层/h. 通过热退火方法得到的多层二维TMDs晶体质量和表面粗糙度不会有较大变化. 但是该方法目前还不成熟, 并非严格按照逐层的方式来减薄, 并且很难得到各向同性的表面.

## 1.2 “自下而上”生长模式

“自上而下”的二维层状材料制备模式经过十多年发展已经成为成熟的实验室手段, 但仍然存在着诸如制备尺寸较小(通常<100 μm)、缺乏可重复性、相对产量较低等缺点, 并不适用于规模化合成, 现阶段只能用于基础研究以及新器件验证等科研领域. 而与之相对的“自下而上”生长模式, 由于其合成机理的本质区别, 更适合制备空间均一性好、厚度可控的大面积二维原子晶体. “自下而上”生长模式可以根据合成方法和生长设备的不同进行细分, 包括CVD[76]、原子层沉积(atomic layer deposition, ALD)、MBE[77]等. 综合比较, CVD法具有生产成本低、合成尺寸大、合成质量好等优点, 在二维层状材料的产业化领域有巨大潜力, 本文将结合二维TMDs的最新研究成果, 重点介绍CVD法.

CVD法利用含有二维层状材料组分的单质或化合物(气相或固相)在预设位置衬底上进行化合反应合成薄膜的生长方法, 该方法具有设备简单、成本低、参数易于调控等优势. 对于单质二维层状材料, 如石墨烯、黑磷、硼烯等材料, 主要根据二元相图选择合适的催化基底或模板, 以及合适的反应物浓度和反应温度, 调控材料的生长或析出条件. 其中单层石墨烯材料CVD生长的探索已经较为成熟, 凭借其在金属镍(Ni)或铜(Cu)表面上生长时具有的自限制特性, 目前已经能够生长大面积、高质量且均一连续的石墨烯薄膜[78~83]. 但与单质的石墨烯不同, 二维TMDs双组分二维原子晶体的CVD生长不具备这种自限制特性, 所以难以简单复制石墨烯的生长方法, 而且二维TMDs材料在CVD生长过程中难以控制其水平和垂直方向上的生长速率, 而水平和垂直方向

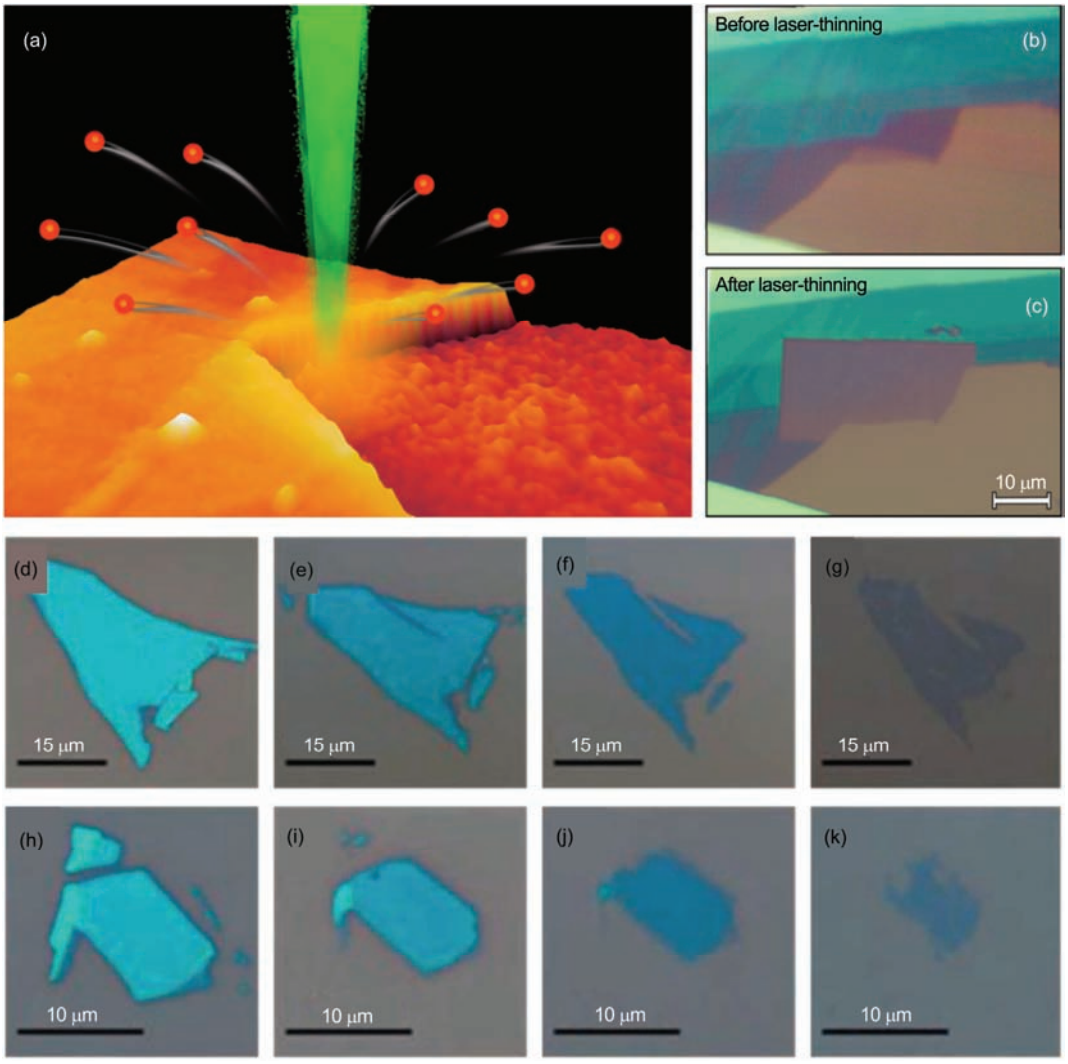


**图 4** (网络版彩色)激光热剥蚀和热退火制备$MoS_2$薄片. (a) 激光热剥蚀制备单层$MoS_2$的示意图; 激光热剥蚀之前(b)和之后(c)的$MoS_2$薄片光学显微镜照片[74]. (d), (h) 退火前$MoS_2$薄片的光学显微镜照片; 退火 2 h((e), (i)), 4 h((f), (j))和 7 h((g), (k))后的光学显微镜照片[75]

**Figure 4** (Color online) Preparation of $MoS_2$ sheets by thermal ablation by laser-thinning. (a) The schematic of laser ablation for thinning $MoS_2$. Optical microscopy images of a multilayered $MoS_2$ flake deposited onto a 285 nm $SiO_2$/Si substrate (b) and after scanning a laser (c)[74]. (d), (h) Optical microscopy images of the pristine $MoS_2$ flake before anneal, and thermal annealed $MoS_2$ flakes. The annealing times are 2 h((e), (i)), 4 h((f), (j)) and 7 h ((g), (k))[75]

上生长速率的比值对晶粒尺寸、薄膜厚度和均一度等方面都有着重要影响, 这使得CVD法获得大尺寸高质量的TMDs薄膜仍然具有一定挑战[84,85].

近年来TMDs的CVD生长也取得了一定的突破和进展, 已陆续有研究结果表明, 使用CVD法能够制备出晶圆级别尺寸的单层连续二维TMDs薄膜、同时其迁移率可以和微机械剥离法等"自上而下"生长模式获得的薄膜相当[86,87]. 总体来说, 常用的CVD法薄膜沉积技术可以分为3种: (1) 热蒸汽硫化(thermal vapor chalcogenization, TVC), 如图5(a), (b)所示, 即首先在衬底上沉积含有目标薄膜组分的源材料化合物或单质薄膜, 然后在X(X=S, Se等)热蒸汽环境中进行硫属化; (2) 热气相沉积(thermal vapor deposition, TVD),如图5(c)所示, 即通过高温加热使前驱体源升华成为气态并随载气流动, 最终在目标衬底上发生直接化合反应来生长二维TMDs薄膜[88,89]; (3) 气相源二维TMDs薄膜的CVD生长, 如图5(d)所示, 反应源材料均为气相源, 通过对反应腔内气相源材料浓度和流量的精确控制, 可以在目标衬底上合成出结晶状况好的高质量、大尺寸连续二维薄膜.

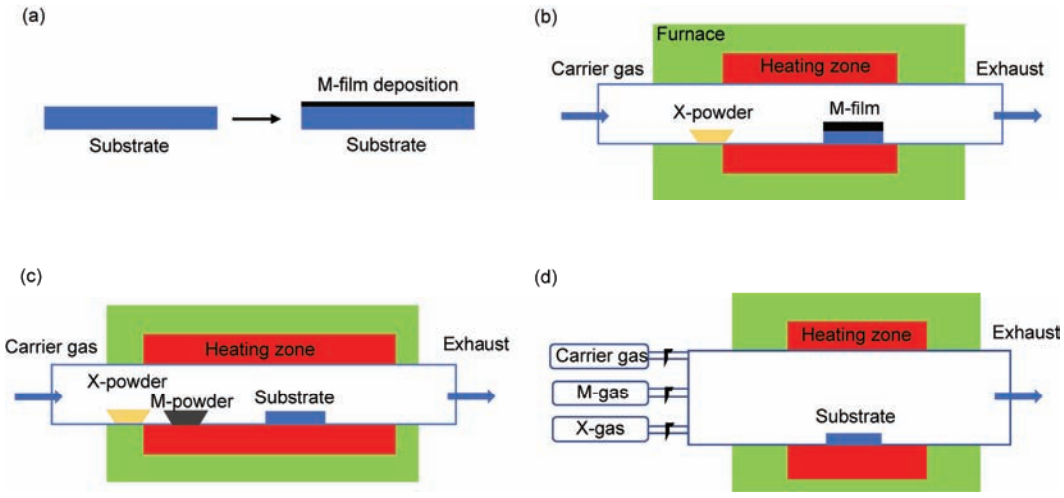


**图5** (网络版彩色)常用CVD法TMD薄膜沉积技术示意图. (a), (b) 典型TVC合成方法示意图, 其中"M-film"代表沉积的过渡金属的化合物或单质薄膜, "X-powder"代表硫族元素的单质粉体; (c) 典型TVD合成方法示意图, 其中"M-powder"代表硫族元素的单质或化合物粉体; (d) 典型纯气相源TMDs薄膜的CVD法合成示意图

**Figure 5** (Color online) Schematic diagrams of CVD methods for preparation of 2D TMDs. (a), (b) Typical processes employed for TVC processes. (c) A typical set-up employed for TVD processes. (d) A typical set-up employed for CVD methods with pure gas sources

### 1.2.1 热蒸汽硫属化

TVC二维层状材料制备方法主要包含两步工艺, 如图5(a), (b)所示, 第1步是在目标衬底上沉积1层含有过渡金属组分的化合物或单质薄膜, 第2步是将沉积薄膜后的衬底置于硫族蒸气环境中(如S或Se蒸气)并加热至预设的温度进行硫属化.

根据所沉积的源材料薄膜是化合物还是单质, 可以将TVC合成方法再细分为2种. 一种是过渡金属直接进行硫属化. 以$MoS_2$为例, 即先在目标衬底上沉积纳米尺度的Mo金属薄膜, 然后置于硫气氛中在高温下进行$MoS_2$的合成. 反应原理可以用下式简要概括:

$$M+nX=MX_n$$

其中, M为过渡金属元素(Mo, W等), X为硫属元素(S, Se等). 通过这种方法生长出的二维TMDs薄膜, 其厚度和面积大小大致可由目标衬底上预淀积金属薄膜的厚度和尺寸所决定.

另一种TVC方法是对过渡金属前驱体(金属氧化物、硫化物等)进行硫属化. 以$MoO_3$为例, 首先在目标衬底上通过适当方法(热蒸发[90]、磁控溅射[91]以及ALD[92,93]等)沉积一层均匀且易于硫属化的$MoO_3$(或$MoS_2$等其他过渡金属前驱体), 然后置入硫气氛中在一定温度下进行化合反应, 最终形成$MoS_2$薄膜. 在硫属化过程中, 前驱体的转换可以直接通过化学反应形成TMDs[91]; 也可以通过1个两步的热反应. 仍以$MoO_3$为例, 即$MoO_3$在高温还原环境下先转变为$MoO_2$, 然后再进行硫属化反应形成$MoS_2$[90]. 反应原理可以用下式简要概括:

$$MoO_3(s)+H_2(g)\rightarrow MoO_2(s)+H_2O(g)$$

$$MoO_2(s)+2S(g)\rightarrow sMoS_2(s)+O_2(g)$$

Choudhary等人[94]利用磁控溅射在$SiO_2$/Si衬底上沉积了金属Mo的薄膜, 随后在600℃下进行硫化, 并通过控制金属Mo层的厚度获得了不同层数的$MoS_2$薄膜, 制备出的背栅晶体管具有良好的特性, 迁移率达到12.24 $cm^2/(V\ s)$, 开关比约$10^6$. 在二维TMDs薄膜的合成工艺中, 衬底材料的选择对于制备薄膜的质量、均一性等有着重要影响, 随着研究的深入, 人们也尝试了其他的衬底类型, 例如蓝宝石(sapphire)、云母以及$SrTiO_3$等. 相比于$SiO_2$/Si, 它们具有表面更加平整、耐高温等特性, 在TVC方法生长二维TMDs薄膜领域具有更大潜力. Laskar等人[95]通过在蓝宝石衬底上先沉积5 nm的Mo并在900℃下进行硫属化, 成功制备出大面积的$MoS_2$薄膜, 电学测试结果表明其迁移率达到了12 $cm^2/(V\ s)$. Buscema等人[96]研究了不同衬底($SiO_2$, h-BN, 聚合物凝胶膜, 云母以及金等)对于单层$MoS_2$的拉曼光谱及光致发光光谱(PL)的影响. 结果表明衬底类型的不同对于单层$MoS_2$不会引入较大的应力, 但会引起掺杂水平的变化; 同时与$SiO_2$相比, 其他类型衬底均增强了PL光谱, 其中柔性聚合物衬底表现出最大的增强效应, 这些结果表

明了二维TMDs材料应用于柔性透明电子器件的可能性. Bao等人[97]发现, 以聚甲基丙烯酸甲酯(PMMA)为衬底的$MoS_2$晶体管器件显示了更高的迁移率; Chamlagain等人[98]也观察到在室温下聚对二甲苯(parylene-C)衬底上$MoSe_2$的迁移率达到100~160 $cm^2/(V\ s)$, 远高于$SiO_2$衬底上的50 $cm^2/(V\ s)$. 他们将这归因于$SiO_2$衬底表面具有极性光学声子散射, 而在PMMA或parylene-C衬底上几乎不存在这种散射效应. Su等人[99]研究并对比了$SiO_2$及蓝宝石衬底上单层$WS_2$的光电学特性, 结果表明TMDs材料与衬底的耦合程度不仅与衬底类型有关, 还与材料和衬底间的结合程度(即使是相同类型衬底)以及光学测试中的激发波长都有关.

如图6(a)~(e)所示, TVC方法中, 在目标衬底上沉积前驱体(过渡金属单质或化合物)的常用方法包括: 热蒸发(thermal evaporation)[90,100,101]、电子束蒸发(E-beam evaporation)[95,102]、磁控溅射(magnetron-sputtering)[94,96,103,]、原子层淀积(atomic layer deposition, ALD)[92,104]、激光分子束外延(pulsed-laser deposition, PLD)[105~107]、CVD[108]以及浸涂法(dip-coating)[87,109]等, 这些源材料薄膜制备手段都可以在目标衬底上获得大尺寸、厚度可控且均一性良好的薄膜. 总体来说, 通过热蒸发、电子束蒸发及浸涂法制备出的前驱体薄膜, 其均匀性和膜密度要小于通过磁控溅射, ALD, 激光分子外延和CVD获得的薄膜, 但成本更低. 所有这些薄膜制备技术获得的膜层其晶粒尺寸都很小(通常<100 nm), 使得通过硫化制备出的二维TMDs薄膜的晶粒尺寸相应地也很小, 通常会需要进行一些热处理手段来改善其结晶状况、增加其晶粒尺寸. Liu等人[88]比较并总结了主要薄膜沉积技术的特点.

结合各种源材料薄膜沉积技术的特点, 在TVC合成方法中, 制备过渡金属(Mo, W等)薄膜通常使用电子束蒸发或磁控溅射; 沉积过渡金属氧化物($MoO_3$, $WO_3$等)薄膜通常使用热蒸发或ALD, 若沉积薄膜直接为二维TMDs($MoS_2$, $WS_2$等)一般就需要使用ALD或激光分子束外延技术. ALD制备出的薄膜具有高均一性和致密性, 但结晶状况差, 通常是多晶态或非晶, 需要相应的热处理后进行重结晶以改善薄膜质量. Tan等人[92]分别使用$MoCl_5$和$H_2S$作为反应

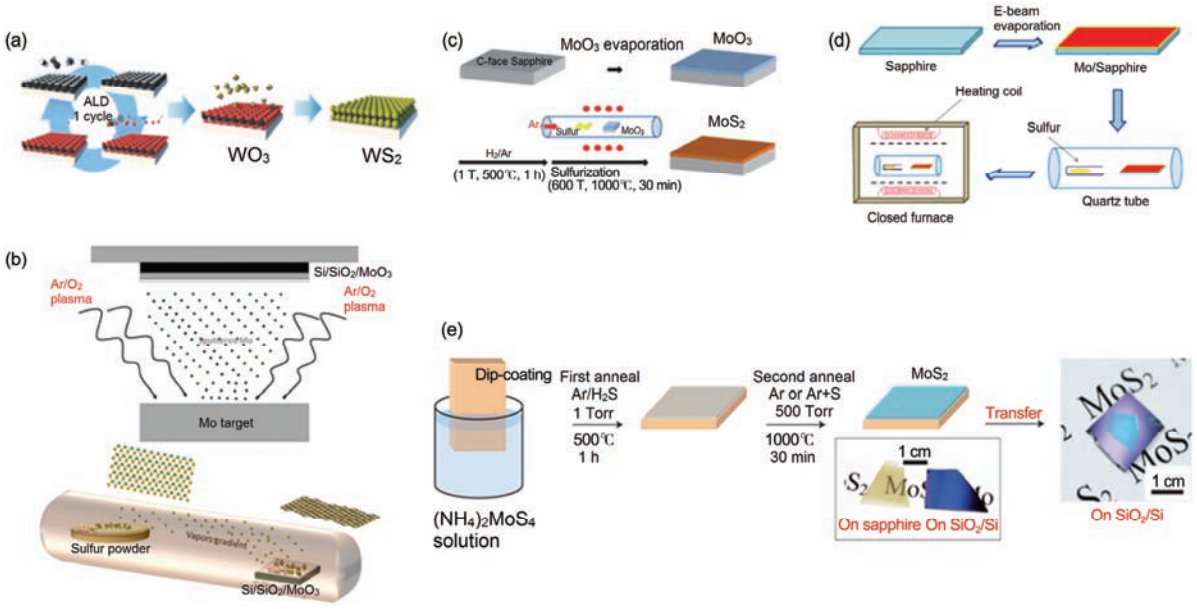


**图 6** (网络版彩色)采用不同前驱体薄膜沉积工艺的TVC合成方法. (a) 通过ALD法预沉积$WO_3$薄膜再硫化得到$WS_2$的示意图[93]; (b) 通过磁控溅射法预沉积$MoO_3$薄膜再硫化得到$MoS_2$的示意图[91]; (c) 通过热蒸发法预沉积$MoO_3$薄膜再硫化得到$MoS_2$的示意图[90]; (d) 通过电子束蒸发法预沉积Mo薄膜再硫化得到$MoS_2$的示意图[95]; (e) 通过浸涂法预沉积前驱体薄膜再两步硫化得到$MoS_2$的示意图[85]

**Figure 6** (Color online) TVC preparation method with various thin-film deposition technologies. (a) Schematic synthetic process of $WS_2$ by sulfurization of ALD deposited $WO_3$[93]. (b) Schematic synthetic process of $MoS_2$ by sulfurization of sputtered $MoO_3$[91]. (c) Schematic synthetic process of $MoS_2$ by sulfurization of thermal evaporated $MoO_3$ film[90]. (d) Schematic synthetic process of $MoS_2$ by sulfurization of e-beam evaporated Mo film[95]. (e) Schematic synthetic process of $MoS_2$ by two-step sulfurization of dip-coated $(NH_4)_2MoS_4$ film[85]

源，在300℃下于目标衬底上制备$MoS_2$薄膜，随后加热至800℃以改善其结晶性. 虽然他们的工作尚不能证明薄膜的连续性，但是为使用ALD制备二维原子晶体薄膜打开了一条新道路. 同时Jin等人[110]使用$Mo(CO)_6$和二甲基二硫化物($CH_3SSCH_3$)作为Mo和S的前驱体，在100℃下制备出高均匀性的$MoS_2$，随后升温至900℃进行热退火以改善其结晶性.

综合来说，TVC合成方法的优势是能够获得大面积、空间均一性好的TMDs原子层，并且在膜层沉积阶段可以很好地控制硫属化和掺杂[111]，但现阶段限制其应用的主要原因是难以获得高迁移率和较大晶粒尺寸，也因此限制了其在实际生产和特定应用领域的发展.

### 1.2.2 热气相沉积

热气相沉积法(TVD)制备二维TMDs薄膜与TVC的发展几乎同步，图7(a)~(c)和(f)展示了几种典型的TVD合成方法的工艺流程. 以图7(c)中的$MoS_2$合成为例，将硫粉、$MoO_3$粉末和目标衬底依次置于反应石英管中，其中衬底相对于Mo源的位置，对于最终沉积的$MoS_2$薄膜的形状、产率和结晶质量有非常大的影响，制备出的$MoS_2$薄膜如图7(d)，(e)所示. 这种合成方法从微观上可以分为4个步骤：(1) 将粉末状的源材料通过加热蒸发或升华进入到载气中；(2) 通过一定速率的载气输送反应物质(通常为Ar或$N_2$等惰性气体)，同时还原反应也可能在该阶段进行；(3) 反应物生成并扩散到预设的目标衬底上；(4) 吸附的源物质在衬底上进行扩散迁移，并继续通过反应或再蒸发后与反应副产物随载气一同排出[88].

由TVD制备方法的反应机理可以看出，目标衬底的物理特性和化学组成对反应物质的吸附、扩散、表面反应、成核及沉积过程有着重要影响，最终决定了制备出的薄膜质量[115,116]. 因此，近年来，研究者对目标衬底的表面处理和形貌设计投入了大量精力，目标是获得更有利于二维TMDs成核和沉积的生长条件，最终获得大尺寸、结晶质量高以及空间均一性好的薄膜. 而目前对于衬底的处理方式主要有2种：

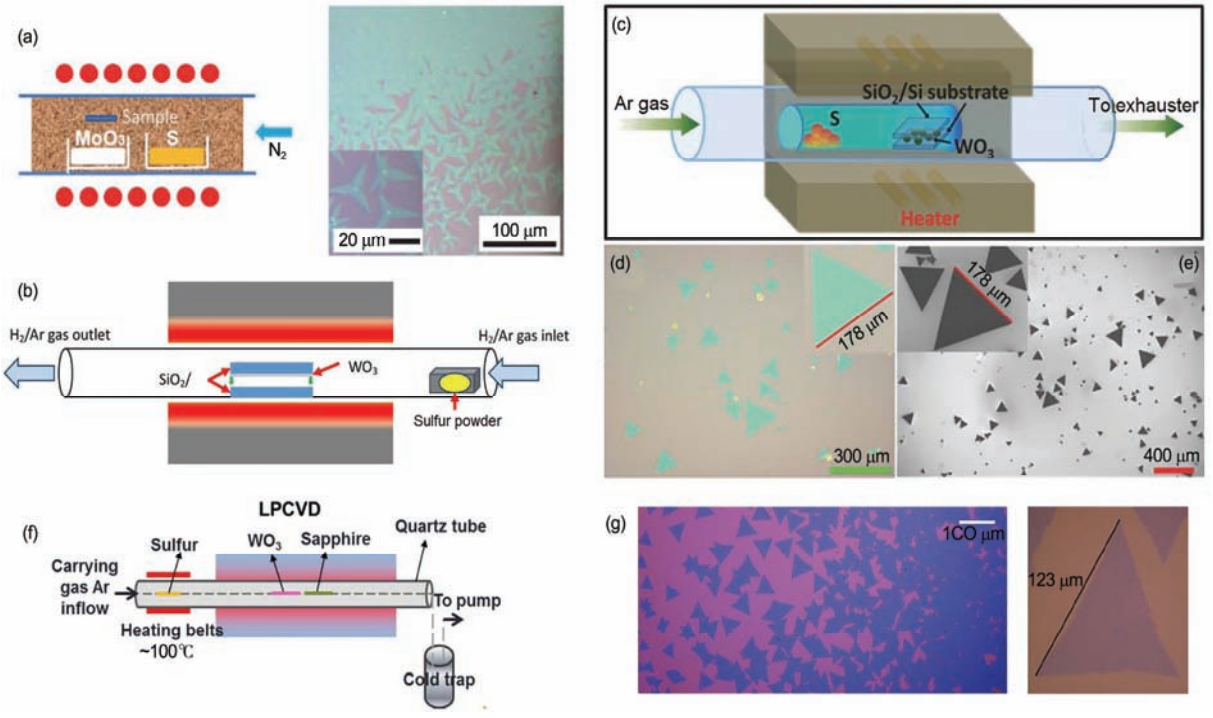


**图 7** (网络版彩色)TVD合成法制备二维TMDs薄膜. (a) $MoO_3$与S粉体制备$MoS_2$的典型实验装置(左)以及光学显微镜下制备的$MoS_2$薄片(右)[85]; (b) $WO_3$与S粉体制备$WS_2$的典型CVD实验装置[101]; (c) $SiO_2$/Si衬底上制备$WS_2$的典型实验装置及光学显微镜(d)和扫描电子显微镜(SEM)(e)照片[112]; (f) 蓝宝石衬底上低压CVD(LPCVD)法制备$WS_2$的典型实验装置[113]; (g) $SiO_2$/Si衬底上制备的大晶粒尺寸的$MoS_2$薄膜光学显微镜图[114]

**Figure 7** (Color online) TVD preparation method for 2D TMDs. (a) Schematic illustration of an experimental set-up (left), and an optical image of obtained $MoS_2$ flakes (right)[85]. (b) A typical set-up for the synthesis of $WS_2$ by $WO_3$ and S powder[101]. (c) A typical set-up for the synthesis of $WS_2$ on $SiO_2$/Si substrate and corresponding images obtained by optical microscope (d) and SEM (e)[112]. (f) A typical set-up of the LPCVD system for synthesis of $WS_2$ on sapphire[113]. (g) Optical images of $MoS_2$ on $SiO_2$/Si substrate with large grain size[114]

第1种是衬底表面成核点的培养, 如Lee等人[117]研究发现通过旋转注入成核促进剂(如氧化石墨烯(rGO), PTAS, PTCDA)预处理目标衬底, 有利于诱导$MoS_2$生长过程中的有效成核和层状生长. 但Najmaei等人[84]在未处理的$SiO_2$/Si衬底上也成功制备边长为10 μm大小的三角形$MoS_2$薄片, 这也表明成核促进剂对于二维TMDs薄膜的初始化生长并不一定是必须的. 第2种是使用等离子气体(如氧)对目标衬底表面进行预处理, Am等人[114]在不引入成核促进剂和衬底表面图案化处理的情况下, 首先使用丙酮、异丙醇和$H_2SO_4$/$H_2O_2$(3∶1)仔细地清洗衬底, 之后通过使用氧等离子体对衬底表面进行预处理, 并最大化减小衬底和前驱体在空气中的暴露时间, 成功生长出晶粒尺寸为120 μm的单层$MoS_2$, 合成出的薄膜在光学显微镜下如图7(g)所示.

除衬底预处理外, TVD合成过程中前驱体材料的选择也是至关重要的, 以$MoS_2$为例, 在不同的研究工作中, 通常以高纯S粉为硫源, 而Mo源的选择包括$MoO_3$和$MoCl_5$等[118]. 不同源材料的选择对最终制备的$MoS_2$薄膜形态有不同的影响. 研究表明, 以$MoO_3$为Mo源可以制备结晶性良好、成三角形的单层$MoS_2$, 但仍缺乏制备均一性好且空间尺度大的薄膜[119]; 而以$MoCl_5$为Mo源则能够制备均匀性好、可控性高的大面积薄膜[120]. 除此之外, 结晶形的$MoO_2$可以直接和硫反应形成二维$MoS_2$薄膜[121]. 而Wu等人[122]使用了一种无催化剂蒸气-固体生长机制的TMDs薄膜合成方法, 即将高纯度的$MoS_2$粉末在650℃下通过简单的物理气相沉积(PVD), 在目标衬底上生长出晶粒尺寸为20 μm的$MoS_2$, 为二维TMDs合成提供了新思路.

除了上述提到的衬底预处理和源材料的选择外, 两种反应物在高温升华后, 气相输运过程中的浓度比, 对于合成出的二维TMDs薄膜质量也有着重要影响. 反应物的浓度比与两种反应物之间的距离、反应物的量、硫粉(或硒粉)的加热温度以及载气的流速等许多因素有关[123]. Wang等人[124]研究了前驱体Mo与S不同浓度比下的$MoS_2$单晶生长形态. 假设$MoS_2$单晶从正六角核开始生长, 紧接着Mo与S原子交替形成六角形的三边, 在此理论下, Mo与S各自生长速率的不同会导致最终形成不同的$MoS_2$晶体形状. 具体来说, Mo∶S生长速率比大于1∶2时生长形成正三角形; 等于1∶2时形成正六角形; 小于1∶2时形成倒三角形. 但是实际生长过程中, 缺陷等其他因素也会导致$MoS_2$单晶呈现除三角形和正六角形以外的不规则形状. 因此要实现二维TMDs薄膜的可控生长其关键点在于能够有效控制随载气输运的两种气相反应物在目标衬底上成核、生长期间的浓度比, 尽管现阶段已对TVD合成法进行了大量研究, 但仍需要进一步深入研究如何控制这一过程.

通过TVD法制备出的二维TMDs薄膜, 其成膜形态、生长速率和结晶状况与生长温度、反应腔几何尺寸、压强、载气流速、源材料的用量和纯度, 以及源材料与目标衬底之间的距离等许多因素相关[115,125~128]. 另外, 与TVC方法不同的是, TVD方法更倾向于获得具有较大晶粒尺寸且高质量的二维TMDs单晶, 但在空间均一性和面积尺度上仍有许多挑战需要去克服. 由于其生长条件的优化和调控也比较复杂, 很大程度上更依赖经验性积累, 可重复性欠缺, 尚不能满足工业化生产的需求.

#### 1.2.3 纯气相源CVD和金属有机化合物化学气相沉淀(MOCVD)

TMDs的气相源CVD生长简要工艺方法如图8(a)~(c)所示, 与传统CVD工艺不同的是, 所有的反应源均采用气相源, 每种源可以单独调控. 这种生长方法的优点在于各个气相源的流量及温度可以同时单独控制, 与生长温度和腔内压强的调控结合后, 可以更好地研究二维TMDs薄膜的生长机制. 这种更加精细的生长调控能力, 也可以用于能带工程研究中的异质结或多元结金化生长. Kranthi等人[129]采用图8(a)所示的气相源CVD生长模式, 其中Mo源使用$Mo(CO)_6$, 而S源使用$H_2S$, 研究了不同生长温度(350~850℃)、不同沉积时间(10 s~10 min)以及不同载气流量等生长参数的影响; 生长完成后保持在$H_2S$气氛中约10 min, 制备出的$MoS_2$薄膜其晶粒尺寸达到20 μm, 室温下迁移率为2.4 $cm^2/(V\,s)$.

通过更加复杂的MOCVD法, Kang等人[86]利用$Mo(CO)_6$为Mo源, $(C_2H_5)_2S$为S源, 550℃下在$SiO_2$/Si衬底上制备出4英寸晶圆级且高质量的单层$MoS_2$薄膜(图8(c)), 展示出极好的空间均匀性以及良好的电学性能(图8(d)). 其器件在室温下迁移率达到30 $cm^2/(V\,s)$, 在90 K的低温下迁移率达到114 $cm^2/(V\,s)$, 该研究是迈向晶圆级二维TMDs制备的重要一步.

综上所述, 在大面积二维TMDs薄膜的各种CVD生长方法中, 衬底条件、源材料选择以及生长工艺参数的变化对于制备出的二维TMDs晶体质量有着重要

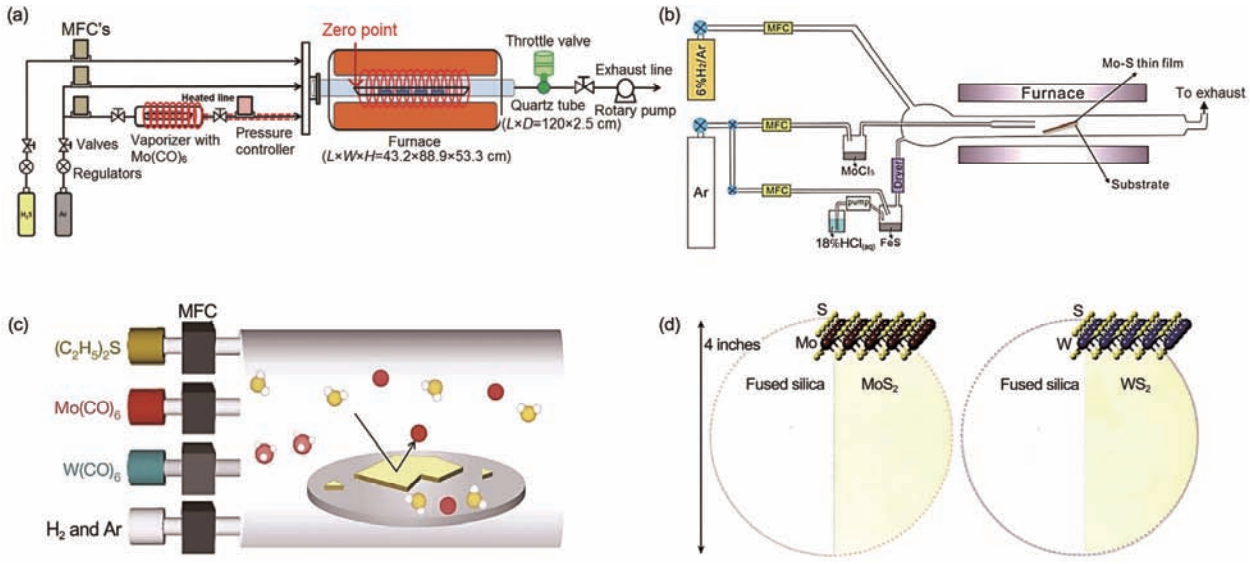


**图 8** (网络版彩色)二维TMDs薄膜的纯气相源的CVD生长和MOCVD工艺. (a), (b) 不同前驱体源的气相法CVD制备$MoS_2$的实验装置原理图[108,129]; (c) MOCVD法制备连续$MoS_2$和$WS_2$薄膜的生长原理图; (d) 4 英寸石英衬底上生长$MoS_2$和$WS_2$薄膜示意图[86]

**Figure 8** (Color online) Illustration of gas-source CVD and MOCVD for preparation of 2D TMDs. (a), (b) Typical set-ups for the synthesis of $MoS_2$ by gas-source CVD with different precursors[108,129]. (c) Schematic diagram showing the growth of continuous $MoS_2$ and $WS_2$ films by MOCVD. (d) Optical images of monolayer $MoS_2$ and $WS_2$ grown on 4-inch fused silica substrates[86]

影响. 与TVC或TVD合成工艺相比, 纯气相源CVD生长在控制二维TMDs的生长重复性、及空间均一性等方面具有良好的发展潜力和应用价值. 此外, MOCVD方法在精确调控和大面积生长方面均有较大的优势, 是极有前景的一种制备二维TMDs薄膜的方法, 但其仍面临着生长周期长、成本高、设备调控复杂等挑战.

### 1.3 “自上而下”与“自下而上”生长模式总结

综上所述, “自上而下”生长模式目前只作为晶圆级大面积生长的补充和延续, 并不具备规模生产的实际应用条件; 而“自下而上”生长模式更适合工业生产和实际应用需求. 目前大部分二维TMDs材料“自下而上”的生长仍然面临着2个重大挑战: (1) 仍需要对生长面积、晶粒尺寸、薄膜连续性、空间均一性以及厚度一致性等进一步优化, 同时降低成本, 并探索相对低温的生长; (2) 实际应用中通常需要特定基底材料来支撑获得的二维TMDs薄膜, 因此需要相应的转移工艺将其剥离到所需的基底上, 但复杂的转移过程与标准CMOS工艺兼容性差, 不可避免地引入薄膜缺陷、破裂和褶皱等问题. 在解决“自下而上”生长方法的这些问题之前, 实际过程中往往需要在某些性能上做一些折中.

## 2 二维TMDs在电子器件中的应用

除了实现二维层状材料的大面积生长, 还需要与微纳电子器件工艺相结合, 才能够实现他们在电子和光电信息器件中的真正应用. 近年来, 随着硅晶体管尺寸的不断缩小, 即将达到其物理极限, 二维层状材料的出现引起了学术界的广泛关注. 例如石墨烯拥有远高于体硅的迁移率以及抑制短沟道效应的能力, 在未来集成电路产业中具有非常重要的战略意义, 但是石墨烯的零禁带宽度特性限制了其在电子器件领域的应用[130~133]. 相比较而言, 二维TMDs材料拥有较大的禁带宽度范围, 可以选取具有理想禁带宽度的材料来保证迁移率、开关比、亚阈值摆幅和阈值电压等各项性能较为均衡[18,134~136]; 同时, 原子级别的沟道厚度也具有较强的抑制短沟道效应能力. 针对近期研究, 表2对基于以上制备手段的TMDs场效应晶体管器件的各种性能进行了归纳.

目前TMDs电子器件研究已经从单个机械剥离的二维原子晶体场效应管性能展示, 发展到光电探测器[145]、传感器[146~148]以及较为复杂的反相器和各种逻辑门[149,150]. 近期, 麻省理工学院和维也纳大学的研究者还利用大面积生长的二维TMDs进行了复杂逻辑电路的初步尝试. FinFET的发明者加州大学伯克利分校胡正明教授也非常看好二维层状材料在

**表 2 不同二维TMDs材料制备方法及其器件性能的总结**

**Table 2** Summary of different 2D-TMDs synthesis methods and corresponding device qualities

| 合成方法 | 材料 | 晶粒/薄膜尺寸 | 导电类型 | 电流开关比 | 迁移率($cm^2$/(V s), 室温) | 文献 |
|---|---|---|---|---|---|---|
| 微机械剥离法 | $MoS_2$ | 几~几十微米 | N | ~$10^8$ | (单层)~200<br>(多层)~500 | [137]<br>[138] |
| | $MoSe_2$ | 几~几十微米 | N | >$10^6$ | (多层)~50 | [139] |
| | $WSe_2$ | 几~几十微米 | N/P | >$10^6$ | (单层, N型)~202<br>(单层, P型)~250 | [140]<br>[141] |
| | $WS_2$ | 几~几十微米 | N | ~$10^6$ | (多层)60 | [142] |
| 液相超声剥离法 | $MoS_2$ | 亚微米<br>网状结构薄膜 | N | >10 | (多层)~0.01 | [69] |
| 激光热剥蚀法 | $MoS_2$ | 几十微米(可控) | N | >$10^3$ | (单层)0.04~0.49 | [74] |
| TVC | $MoS_2$ | 连续薄膜 | N | ~$10^4$ | ~0.004~0.04 | [102] |
| | | 连续薄膜 | N | ~$10^5$ | ~0.8 | [90] |
| | | 非连续薄膜 | N | ~$10^4$~$10^6$ | ~0.1~0.7 | [121] |
| | | 5~20 μm<br>连续薄膜 | N | ~$10^5$ | ~6 | [87] |
| | $WS_2$ | 约几十纳米<br>非连续薄膜 | –[a)] | –[a)] | –[a)] | [143] |
| | | 5~15 μm<br>连续薄膜<br>10~20 nm | N | ~$10^3$ | ~3.9 | [104] |
| TVD | $MoS_2$ | 非连续薄膜 | N | ~$10^4$ | ~0.02 | [31] |
| | | 约160 nm<br>连续薄膜 | N | ~$10^5$~$6\times10^6$ | ~0.2~18 | [89] |
| | | 约几十微米<br>非连续薄膜 | N | ~$10^5$~$10^7$ | ~1~8 | [114] |
| | | 约123 μm<br>连续薄膜 | N | ~$10^3$ | ~0.003~0.03 | [118] |
| | $WS_2$ | 非连续薄膜 | N | ~$10^5$ | ~0.01 | [117] |
| | | 约10 μm<br>非连续薄膜 | – | – | – | [112] |
| | | 约178 μm<br>非连续薄膜 | 双极 | ~$10^2$ | ~0.28~0.46 | [113] |
| | $MoSe_2$ | 约50 μm<br>非连续薄膜<br>1.3~1.6 mm | N | ~$10^5$~$10^7$ | ~42 | [144] |
| 气相源CVD | $MoS_2$ | 非连续薄膜 | N | ~$10^5$ | ~2.4~7.1 | [129] |
| | | 约25 μm<br>连续薄膜<br>100 nm~10 μm | N | ~$10^6$ | ~10~40 | [86] |
| | $WS_2$ | 连续薄膜<br>100 nm~10 μm | N | ~$10^6$ | ~5~18 | [86] |

a): “–”表示文献未给出明确数值

存储和逻辑器件方向的应用前景, 他领导的研究小组已经实现了基于二维TMDs材料的互补逻辑电路[151]. 同时, 新原理器件也不断涌现, 例如基于二维层状材料的隧穿场效应晶体管和负电容效应逻辑器件[152], 两者都有极陡峭的开关电压转换, 可以满足低功耗高速逻辑器件的需求.

## 3 总结与展望

自2004年以来, 以石墨烯、TMDs等材料为代表的二维层状材料不断地被重新认识并合成出来, 其

物理性质涵盖了金属、半导体和绝缘体的范畴. “自上而下”的制备方法简单实用, 普遍用于材料的基本物理化学性质的研究和原型器件的展示. “自下而上”的方法则更适合晶圆级大面积高质量的材料制备, 其中, CVD法制备二维TMDs材料近几年来取得了快速发展, 但存在着一系列亟待解决的关键问题, 包括选择合适的生长基底, 调控不同组分的扩散次序、浓度、压力、时间等条件, 解析大尺寸晶畴的生长条件, 以及发展异质结构的交替生长方法等. 此外, 与材料性质息息相关的无损低残留大面积转移以及低温无转移生长等方法也是关键研究内容.

未来, 国际半导体行业已经确定不再以摩尔定律为基调制定路线图, 而是基于现实需求提出“超摩尔战略”来开启未来半导体新的增长点, 对今后新材料和新器件的研发提出了更多要求. 在此背景下, 二维TMDs半导体材料的兴起为新型信息器件发展提供了良好机遇. 探索“自下而上”制备方法的合成机理以及拓展这类方法的适用性, 并制备用以工业化的二维TMDs材料, 是今后几年内的发展核心; 在此基础上, 与实际应用息息相关的器件结构、工艺、性能优化等一系列问题也是迫切需要解决的. 总的来说, 只有妥善处理并协调好“材料基础特性-生长合成机理-器件工艺”三者之间的关系, 才能为未来二维TMDs的发展和应用做好充分准备.

## 参考文献


1 Geim A K, Novoselov K S. The rise of graphene. Nat Mater, 2007, 6: 183–191
2 Novoselov K S, Geim A K, Morozov S V, et al. Electric field effect in atomically thin carbon films. Science, 2004, 306: 666–669
3 Zhang Y, Tan Y W, Stormer H L, et al. Experimental observation of the quantum Hall effect and Berry’s phase in graphene. Nature, 2005, 438: 201–206
4 Dean C R, Young A F, Meric I, et al. Boron nitride substrates for high-quality graphene electronics. Nat Nanotechnol, 2010, 5: 722–726
5 Schwierz F. Graphene transistors. Nat Nanotechnol, 2010, 5: 487–496
6 Ugeda M M, Bradley A J, Shi S F, et al. Giant bandgap renormalization and excitonic effects in a monolayer transition metal dichalcogenide semiconductor. Nat Mater, 2014, 13: 1091–1097
7 Tan C, Zhang H. ChemInform abstract: Two-dimensional transition metal dichalcogenide nanosheet-based composites. Chem Soc Rev, 2015, 44: 2713–2731
8 Bhattacharyya S, Singh A K. Semiconductor-metal transition in semiconducting bilayer sheets of transition-metal dichalcogenides. Phys Rev B, 2012, 86: 075454
9 Lu J, Zheliuk O, Leermakers I, et al. Evidence for two-dimensional Ising superconductivity in gated $MoS_2$. Science, 2015, 350: 1353–1357
10 Terrones H, Terrones M. Electronic and vibrational properties of defective transition metal dichalcogenide Haeckelites: New 2D semi-metallic systems. 2D Mater, 2014, 1: 011003
11 Chhowalla M, Shin H S, Eda G, et al. The chemistry of two-dimensional layered transition metal dichalcogenide nanosheets. Nat Chem, 2013, 5: 263–275
12 Zhao W, Ghorannevis Z, Chu L, et al. Evolution of electronic structure in atomically thin sheets of $WS_2$ and $WSe_2$. ACS Nano, 2012, 7: 791–797
13 Mak K F, Lee C, Hone J, et al. Atomically thin $MoS_2$: A new direct-gap semiconductor. Phys Rev Lett, 2010, 105: 136805–136809
14 Ghorbani-Asl M, Borini S, Kuc A, et al. Strain-dependent modulation of conductivity in single-layer transition-metal dichalcogenides. Phys Rev B, 2013, 87: 235434
15 Wang Y, Cong C, Yang W, et al. Strain-induced direct–indirect bandgap transition and phonon modulation in monolayer $WS_2$. Nano Res, 2015, 8: 2562–2572
16 He J, Hummer K, Franchini C. Stacking effects on the electronic and optical properties of bilayer transition metal dichalcogenides $MoS_2$, $MoSe_2$, $WS_2$, and $WSe_2$. Phys Rev B, 2014, 89: 520–531
17 Song X, Guo Z, Zhang Q, et al. Progress of large-scale synthesis and electronic device application of two-dimensional transition metal dichalcogenides. Small, 2017, 13: 1700098
18 Franklin A D. Device technology. Nanomaterials in transistors: From high-performance to thin-film applications. Science, 2015, 349: 2750–2755
19 Manzeli S, Ovchinnikov D, Pasquier D, et al. 2D transition metal dichalcogenides. Nature, 2017, 2: 17033–17040
20 Yu Z, Ong Z Y, Li S, et al. Analyzing the carrier mobility in transition-metal dichalcogenide $MoS_2$ field-effect transistors. Adv Funct Mater, 2017, 27: 1–61

21 Zhao Y, Xu K, Pan F, et al. Doping, contact and interface engineering of two-dimensional layered transition metal dichalcogenides transistors. Adv Funct Mater, 2017, 27: 1603484

22 Zhang S, Xie M, Li F, et al. Semiconducting group15 monolayers: A broad range of band gaps and high carrier mobilities. Angew Chem Int Ed, 2016, 128: 1666–1669

23 Peng B, Yu G, Liu X, et al. Ultrafast charge transfer in $MoS_2$/WSe p-n heterojunction. 2D Mater, 2016, 3: 025020–025032

24 Wang J, Yao Q, Huang C W, et al. High mobility $MoS_2$ transistor with low schottky barrier contact by using atomic thick H-BN as a tunneling layer. Adv Mater, 2016, 28: 8302–8308

25 Buscema M, Island J O, Groenendijk D J, et al. Photocurrent generation with two-dimensional van der Waals semiconductors. Chem Soc Rev, 2015, 44: 3691–3718

26 Liu Y, Weiss N O, Duan X, et al. Van der Waals heterostructures and devices. Nature, 2016, 1: 16042–16048

27 Novoselov K S, Mishchenko A, Carvalho A, et al. 2D materials and van der Waals heterostructures. Science, 2016, 353: 9439

28 Benka S G. Two-dimensional atomic crystals. Proc Natl Acad Sci USA, 2005, 102: 10451–10453

29 Eda G, Yamaguchi H, Voiry D, et al. Photoluminescence from chemically exfoliated $MoS_2$. Nano Lett, 2011, 11: 5111–5116

30 Nicolosi V, Chhowalla M, Kanatzidis M G, et al. Liquid exfoliation of layered materials. Science, 2013, 340: 1420

31 Lee Y H, Zhang X Q, Zhang W, et al. Synthesis of large-area $MoS_2$ atomic layers with chemical vapor deposition. Adv Mater, 2012, 24: 2320–2325

32 Xu G C, Lu Z X, Zhang Q, et al. Synthesis of two-dimensional transition metal dichalcogenides with chemical vapor deposition (in Chinese). Acta Chim Sin, 2015, 73: 895–901 [许冠辰, 卢至行, 张琪, 等. 化学气相沉积法合成二维过渡金属硫族化合物研究进展. 化学学报, 2015, 73: 895–901]

33 Frindt R F. Single crystals of $MoS_2$ several molecular layers thick. Appl Phys, 1966, 37: 1928–1929

34 Lu X, Yu M, Huang H, et al. Tailoring graphite with the goal of achieving single sheets. Nanotechnology, 1999, 1099: 269–272

35 Zhang Y, Small J P, Pontius W V, et al. Fabrication and electric-field-dependent transport measurements of mesoscopic graphite devices. Appl Phy Lett, 2004, 86: 073104

36 Gupta A, Sakthivel T, Seal S. Recent development in 2D materials beyond graphene. Prog Mater Sci, 2015, 73: 44–126

37 Wang G, Bao L, Ma R, et al. From bidirectional rectifier to polarity-controllable transistor in black phosphorus by dual gate modulation. 2D Mater, 2017, 4: 025056

38 Li L, Yu Y, Ye G J, et al. Black phosphorus field-effect transistors. Nat Nanotechnol, 2014, 9: 372–377

39 Liu C S, Zhou P, Zhang W. Atomic crystal nonvolatile storage (in Chinese). Sci Sin Phys Mech Astron, 2016: 107308 [刘春森, 周鹏, 张卫. 原子晶体非易失存储. 中国科学: 物理学 力学 天文学, 2016: 107308]

40 Late D J, Shirodkar S N, Waghmare U V, et al. Thermal expansion, anharmonicity and temperature-dependent Raman spectra of single- and few-layer $MoSe_2$ and $WSe_2$. Chem Phys Chem, 2014, 15: 1592–1598

41 Dines M B. Lithium intercalation via *N*-butyllithium of the layered transition metal dichalcogenides. Mater Res Bull, 1975, 10: 287–291

42 Zhao Y, Qiao J, Yu P, et al. Extraordinarily strong interlayer interaction in 2D Layered $PtS_2$. Adv Mater, 2016, 28: 2399–2407

43 Das S, Prakash A, Salazar R, et al. Toward low-power electronics: Tunneling phenomena in transition metal dichalcogenides. ACS Nano, 2014, 8: 1681–1689

44 Wu C C, Jariwala D, Sangwan V K, et al. Elucidating the photoresponse of ultrathin $MoS_2$ field-effect transistors by scanning photocurrent microscopy. Phys Chem Lett, 2013, 4: 2508–2513

45 Neal A T, Liu H, Gu J, et al. Magneto-transport in $MoS_2$: Phase coherence, spin-orbit scattering, and the Hall factor. ACS Nano, 2013, 7: 7077–7082

46 Li D, Chen M, Sun Z, et al. Two-dimensional non-volatile programmable p-n junctions. Nat Nanotechnol, 2017, 12: 901–906

47 Perkins F K, Friedman A L, Cobas E, et al. Chemical vapor sensing with monolayer $MoS_2$. Nano Lett, 2013, 13: 668–673

48 Yu L, Zubair A, Santos E J G, et al. High-performance $WSe_2$ complementary metal oxide semiconductor technology and integrated circuits. Nano Lett, 2015, 15: 4928–4948

49 Lee J, Wang Z, Xie H, et al. Valley magnetoelectricity in single-layer $MoS_2$. Nat Mater, 2017, 16: 887–891

50 Mak K F, McGill K L, Park J, et al. The valley Hall effect in $MoS_2$ transistors. Science, 2014, 344: 1489–1492

51 Bandurin D A, Tyurnina A V, Yu G L, et al. High electron mobility, quantum Hall effect and anomalous optical response in atomically thin InSe. Nat Nanotechnol, 2017, 12: 223–241

52 Li X, Zhang F, Niu Q. Unconventional quantum Hall effect and tunable spin hall effect in Dirac materials: Application to an isolated $MoS_2$ trilayer. Phys Rev Lett, 2013, 110: 066803

53 Costanzo D, Jo S, Berger H, et al. Gate-induced superconductivity in atomically thin $MoS_2$ crystals. Nat Nanotechnol, 2016, 86: 1301–1320

54 Choe D H, Sung H J, Chang K J. Understanding topological phase transition in transition metal dichalcogenides. Phys Rev B, 2016, 93: 274–274

55 Joensen P, Frindt R F, Morrison S R. Single-layer $MoS_2$. Mater Res Bull, 1986, 21: 457–461

56 Zhang H, Lu S B, Zheng J, et al. Molybdenum disulfide ($MoS_2$) as a broadband saturable absorber for ultra-fast photonics. Opt Express, 2014, 22: 7249–7260

57 Huang X, Zeng Z, Zhang H. Metal dichalcogenide nanosheets: Preparation, properties and applications. Chem Soc Rev, 2013, 42: 1934–1946

58 Zeng Z, Yin Z, Huang X, et al. Single-layer semiconducting nanosheets: High-yield preparation and device fabrication. Angew Chem Int Ed, 2011, 50: 11093–11097

59 Tsai H L, Heising J, Schindler J L, et al. Exfoliated-restacked phase of $WS_2$. Chem Mater, 1997, 9: 879–882

60 Bissessur R, Kanatzidis M G, Schindler J L, et al. Encapsulation of polymers into $MoS_2$ and metal to insulator transition in metastable $MoS_2$. Phys Rev B, 1993, 29: 849

61 Zeng Z, Sun T, Zhu J, et al. An effective method for the fabrication of few-layer-thick inorganic nanosheets. Angew Chem Int Ed, 2012, 51: 9052–9056

62 Matte H S S, Gomathi A, Manna A K, et al. $MoS_2$ and $WS_2$ analogues of graphene. Angew Chem Int Ed, 2010, 49: 4059–4062

63 Smith R J, King P J, Lotya M, et al. Large-scale exfoliation of inorganic layered compounds in aqueous surfactant solutions. Adv Mater, 2011, 23: 3944–3948

64 May P, Khan U, Hughes J M, et al. Role of solubility parameters in understanding the steric stabilization of exfoliated two-dimensional nanosheets by adsorbed polymers. Phys Chem C, 2012, 116: 11393–11400

65 Hernandez Y, Nicolosi V, Lotya M, et al. High-yield production of graphene by liquid-phase exfoliation of graphite. Nat Nanotechnol, 2008, 3: 563–568

66 Khan U, O'Neill A, Lotya M, et al. High-concentration solvent exfoliation of graphene. Small, 2010, 6: 864–885

67 Lotya M, Hernandez Y, King P J, et al. Liquid phase production of graphene by exfoliation of graphite in surfactant/water solutions. J Am Chem Soc, 2009, 131: 3611–3630

68 Zhou K G, Mao N N, Wang H X, et al. A mixed-solvent strategy for efficient exfoliation of inorganic graphene analogues. Angew Chem Int Ed, 2011, 50: 10839–10842

69 Coleman J N, Lotya M, O'Neill A, et al. Two-dimensional nanosheets produced by liquid exfoliation of layered materials. Science, 2011, 331: 568–571

70 Cunningham G, Lotya M, Cucinotta C S, et al. Solvent exfoliation of transition metal dichalcogenides: Dispersibility of exfoliated nanosheets varies only weakly between compounds. ACS Nano, 2012, 6: 3468–3480

71 Hanlon D, Backes C, Doherty E, et al. Liquid exfoliation of solvent-stabilised for black phosphorus: Applications beyond electronics. Nat Commun, 2015, 6: 8563

72 Yasaei P, Kumar B, Foroozan T, et al. High-quality black phosphorus atomic layers by liquid-phase exfoliation. Adv Mater, 2015, 27: 1887–1892

73 Han G H, Chae S J, Kim E S, et al. Laser thinning for monolayer graphene formation: Heat sink and interference effect. ACS Nano, 2011, 5: 263–268

74 Castellanos-Gomez A, Barkelid M, Goossens A M, et al. Laser-thinning of $MoS_2$: On demand generation of a single-layer semiconductor. Nano Lett, 2012, 12: 3187–3192

75 Lu X, Utama M I, Zhang J, et al. Layer-by-layer thinning of $MoS_2$ by thermal annealing. Nanoscale, 2013, 5: 8904–8908

76 Xu C, Wang L, Liu Z, et al. Large-area high-quality 2D ultrathin $Mo_2C$ superconducting crystals. Nat Mater, 2015, 14: 1135–1141

77 Lin X, Lu J C, Shao Y, et al. Intrinsically patterned two-dimensional materials for selective adsorption of molecules and nanoclusters. Nat Mater, 2017, 16: 717–721

78 Li C W. Large-area systhesis of high-quality and uniform graphene films on copper foils. Science, 2009, 324: 1312–1314

79 Wang G, Zhang M, Liu S, et al. Graphene: Synthesis of layer-tunable graphene: A combined kinetic implantation and thermal ejection approach. Adv Funct Mater, 2015, 25: 3796

80 Wang G, Zhang M, Zhu Y, et al. Direct growth of graphene film on germanium substrate. Sci Rep, 2013, 3: 2465–2471

81 Wu T, Zhang X, Yuan Q, et al. Fast growth of inch-sized single-crystalline graphene from a controlled single nucleus on Cu-Ni alloys. Nat Mater, 2016, 15: 43–47

82 Chen Y, Sun J, Gao J, et al. Growing uniform graphene disks and films on molten glass for heating devices and cell culture. Adv Mater, 2016, 27: 7839–7846

83 Xu X, Zhang Z, Dong J, et al. Ultrafast epitaxial growth of metre-sized single-crystal graphene on industrial Cu foil. Sci Bull, 2017, 62: 1074–1080

84 Najmaei S, Liu Z, Zhou W, et al. Vapour phase growth and grain boundary structure of molybdenum disulphide atomic layers. Nat Mater, 2013, 12: 754–759

85 Wang Q H, Kalantar-Zadeh K, Kis A, et al. Electronics and optoelectronics of two-dimensional transition metal dichalcogenides. Nat Nanotechnol, 2012, 7: 699–712

86 Kang K, Xie S, Huang L, et al. High-mobility three-atom-thick semiconducting films with wafer-scale homogeneity. Nature, 2015, 520: 656–660

87 Liu K K, Zhang W, Lee Y H, et al. Growth of large-area and highly crystalline $MoS_2$ thin layers on insulating substrates. Nano Lett, 2012, 12: 1538–1558

88 Liu H F, Wong S L, Chi D Z. ChemInform abstract: CVD growth of $MoS_2$-based two-dimensional materials. Chem Vap Dep, 2016, 47: 241–259

89 Andoshe D M, Jeon J M, Kim S Y, et al. Two-dimensional transition metal dichalcogenide nanomaterials for solar water splitting. Electron Mater Lett, 2015, 11: 323–335

90 Lin Y C, Zhang W, Huang J K, et al. Wafer-scale $MoS_2$ thin layers prepared by $MoO_3$ sulfurization. Nanoscale, 2012, 4: 6637–6641

91 Hussain S, Shehzad M A, Vikraman D, et al. Synthesis and characterization of large-area and continuous $MoS_2$ atomic layers by RF magnetron sputtering. Nanoscale, 2016, 8: 4340–4348

92 Tan L K, Liu B, Teng J H, et al. Atomic layer deposition of a $MoS_2$ film. Nanoscale, 2014, 6: 10584–10588

93 Schwartzberg A M, Olynick D. Complex materials by atomic layer deposition. Adv Mater, 2015, 27: 5778–8457

94 Choudhary N, Park J, Hwang J Y, et al. Growth of large-scale and thickness-modulated $MoS_2$ nanosheets. ACS Appl Mater Interfaces, 2014, 6: 21215–21222

95 Laskar M R, Ma L, Kannappan S, et al. Large area single crystal (0001) oriented $MoS_2$. Appl Phys Lett, 2013, 102: 252108

96 Buscema M, Gary S A, van der Zant H S J, et al. The effect of the substrate on the Raman and photoluminescence emission of single-layer $MoS_2$. Nano Res, 2014, 7: 561–571

97 Bao W, Cai X, Kim D H, et al. High mobility ambipolar $MoS_2$ field-effect transistors. Appl Phy Lett, 2012, 102: 042104

98 Chamlagain B, Li Q, Ghimire N J, et al. Mobility improvement and temperature dependence in $MoSe_2$ field-effect transistors on parylene-C substrate. ACS Nano, 2014, 8: 5079–5088

99 Su L, Yu Y F, Cao L Y, et al. Effects of substrate type and material-substrate bonding on high-temperature behavior of monolayer $WS_2$. Nanotechnol Res, 2015, 8: 2686–2697

100 Cho B, Hahm M G, Choi M, et al. Charge-transfer-based gas sensing using atomic-layer $MoS_2$. Sci Rep, 2015, 5: 8052–8058

101 Kang K N, Godin K, Yang E H. The growth scale and kinetics of $WS_2$ monolayers under varying $H_2$ concentration. Sci Rep, 2015, 5: 13205–13214

102 Zhan Y, Liu Z, Najmaei S, et al. Large area vapor phase growth and characterization of $MoS_2$ atomic layers on $SiO_2$ substrate. Small, 2012, 8: 966–971

103 Liu H F, Antwi K K A, Ying J F, et al. Towards large area and continuous $MoS_2$ atomic layers via vapor-phase growth: Thermal vapor sulfurization. Nanotechnology, 2014, 25: 405702–405739

104 Song J G, Park J, Lee W, et al. Layer-controlled, wafer-scale, and conformal synthesis of tungsten disulfide nanosheets using atomic layer deposition. ACS Nano, 2013, 7: 11333–11340

105 Ho Y T, Ma C H, Luong T T, et al. Layered $MoS_2$ grown on c-sapphire by pulsed laser deposition. Phys Status Solidi Rap Res Lett, 2015, 9: 187–191

106 Loh T A J, Chua D H C, Wee A T S. One-step synthesis of few-layer $WS_2$ by pulsed laser deposition. Sci Rep, 2015, 5: 18116–18125

107 Gao M, Zhang M, Niu W, et al. Tuning the transport behavior of centimeter-scale $WTe_2$ ultrathin films fabricated by pulsed laser deposition. Appl Phys Lett, 2017, 111: 205–210

108 Huang C C, Alsaab F, Wang Y, et al. Scalable high-mobility $MoS_2$ thin films fabricated by an atmospheric pressure chemical vapor deposition process at ambient temperature. Nanoscale, 2014, 6: 12792–12797

109 Mishra A K, Lakshmi K V, Huang L. Eco-friendly synthesis of metal dichalcogenides nanosheets and their environmental remediation potential driven by visible light. Sci Rep, 2015, 5: 15718–15726

110 Jin Z, Shin S, Kwon D H, et al. Novel chemical route for atomic layer deposition of $MoS_2$ thin film on $SiO_2$/Si substrate. Nanoscale, 2014, 6: 14453–14458

111 Xing L, Jiao L Y. Recent advances in the chemical doping of two-dimensional molybdenum disulfide (in Chinese). Acta Phys Chem Sin, 2016, 32: 2133–2145 [邢垒, 焦丽颖. 二硫化钼二维原子晶体化学掺杂研究进展. 物理化学学报, 2016, 32: 2133–2145]

112 Cong C, Shang J, Wu X, et al. Synthesis and optical properties of large-area single-crystalline 2D semiconductor $WS_2$ monolayer from chemical vapor deposition. Adv Opt Mater, 2014, 2: 131–136

113 Zhang Y, Zhang Y, Ji Q, et al. Controlled growth of high-quality monolayer $WS_2$ layers on sapphire and imaging its grain boundary. ACS Nano, 2013, 7: 8963–8971

114 Am V D Z, Huang P Y, Chenet D A, et al. Grains and grain boundaries in highly crystalline monolayer molybdenum disulphide. Nat Mater, 2013, 12: 554–561

115 Ochedowski O, Marinov K, Scheuschner N, et al. Effect of contaminations and surface preparation on the work function of single layer $MoS_2$. Beilstein J Nanotechnol, 2014, 5: 291–298

116 Liu B, Fathi M, Chen L, et al. Chemical vapor deposition growth of monolayer $WSe_2$ with tunable device characteristics and growth mechanism study. ACS Nano, 2015, 9: 6119–6125

117 Lee Y H, Yu L, Wang H, et al. Synthesis and transfer of single-layer transition metal disulfides on diverse surfaces. Nano Lett, 2013, 13: 1852–1858

118 Yu Y, Li C, Liu Y, et al. Controlled scalable synthesis of uniform, high-quality monolayer and few-layer $MoS_2$ films. Sci Rep, 2013, 3: 1866–1872

119 Wu W, De D, Chang S C, et al. High mobility and high on/off ratio field-effect transistors based on chemical vapor deposited single-crystal $MoS_2$ grains. Appl Phys Lett, 2013, 102: 6666–6673

120 Mccreary K M, Hanbicki A T, Robinson J T, et al. Large-area synthesis of continuous and uniform $MoS_2$ monolayer films on graphene. Adv Funct Mater, 2015, 24: 6449–6454

121 Wang X, Feng H, Wu Y, et al. Controlled synthesis of highly crystalline $MoS_2$ flakes by chemical vapor deposition. J Am Chem S: , 2013, 135: 5304–5307

122 Wu S, Huang C, Aivazian G, et al. Vapor-solid growth of high optical quality $MoS_2$ monolayer with near unity valley polarization. ACS Nano, 2013, 7: 2768–2772

123 Zhou C, Zhao Y, Raju S, et al. Carrier type control of $WSe_2$ field-effect transistors by thickness modulation and $MoO_3$ layer doping. Adv Funct Mater, 2016, 26: 4223–4230

124 Wang S, Rong Y, Fan Y, et al. Shape evolution of monolayer $MoS_2$ crystals grown by chemical vapor deposition. Chem Mater, 2014, 26: 6371–6379

125 Jeon J, Jang S K, Jeon S M, et al. Layer-controlled CVD growth of large-area two-dimensional $MoS_2$ films. Nanoscale, 2015, 7: 1688–1695

126 Hu D, Xu G, Xing L, et al. Two-dimensional semiconductors grown by chemical vapor transport. Angew Chem Int Ed, 2017, 129: 3665–3669

127 Fu L, Wang F, Wu B, et al. Van der Waals epitaxial growth of atomic layered $HfS_2$ crystals for ultrasensitive near-infrared phototransistors. Adv Mater, 2017, 29: 1–8

128 Chen J, Zhao X, Tan S J R, et al. Chemical vapor deposition of large-size monolayer $MoSe_2$ crystals on molten glass. J Am Chem Soc, 2017, 139: 1073–1077

129 Kranthi K V, Dhar S, Choudhury T H, et al. A predictive approach to CVD of crystalline layers of TMDs: The case of $MoS_2$. Nanoscale, 2015, 7: 7802–7810

130 Han M Y, Ozyilmaz B, Zhang Y, et al. Energy band gap engineering of graphene nanoribbons. Phys Rev Lett, 2007, 98: 206805

131 Reina A, Jia X, Ho J, et al. Large area, few-layer graphene films on arbitrary substrates by chemical vapor deposition. Nano Lett, 2009, 9: 30–35

132 Zhu Y, Murali S, Cai W, et al. Graphene and graphene oxide: Synthesis, properties, and applications. Adv Mater, 2010, 22: 3906–3924

133 Wang X, Ouyang Y, Li X, et al. Room-temperature all-semiconducting sub-10-nm graphene nanoribbon field-effect transistors. Phys Rev Lett, 2008, 100: 206803–206807

134 Yoon Y, Ganapathi K, Salahuddin S. How good can monolayer $MoS_2$ transistors be? Nano Lett, 2011, 11: 3768–3772

135 Qiu H, Wang X R. Electron transport and devices of molybdenum disulfide (in Chinese). J Nanjing Univ Nat Sci, 2014, 50: 280–293 [邱浩, 王欣然. 二硫化钼的电子输运与器件. 南京大学学报(自然科学), 2014, 50: 280–293]

136 Li J, Sun X, Xu C, et al. Electrical contacts in monolayer blue phosphorene devices. Nano Res, 2017, 1998: 1–16

137 Radisavljevic B, Radenovic A, Brivio J, et al. Single-layer $MoS_2$ transistors. Nat Nanotechnol, 2011, 6: 147–150

138 Liu H, Ye P D. $MoS_2$ dual-gate MOSFET with atomic-layer-deposited $Al_2O_3$ as top-gate dielectric. IEEE Electron Dev Lett, 2012, 33: 546–548

139 Larentis S, Fallahazad B, Tutuc E. Field-effect transistors and intrinsic mobility in ultra-thin $MoSe_2$ layers. Appl Phys Lett, 2012, 101: 193–205

140 Liu W, Kang J, Sarkar D, et al. Role of metal contacts in designing high-performance monolayer n-type $WSe_2$ field effect transistors. Nano Lett, 2013, 13: 1983–1990

141 Fang H, Chuang S, Chang T C, et al. High-performance single layered $WSe_2$ p-FETs with chemically doped contacts. Nano Lett, 2012, 12: 3788–3792
142 Yang L, Majumdar K, Liu H, et al. Chloride molecular doping technique on 2D materials: $WS_2$ and $MoS_2$. Nano Lett, 2014, 14: 6275–6280
143 Gutiérrez H R, Perea-López N, Elías A L, et al. Extraordinary room-temperature photoluminescence in triangular $WS_2$ monolayers. Nano Lett, 2013, 13: 3447–3454
144 Gong Y, Ye G, Lei S, et al. Synthesis of millimeter-scale transition metal dichalcogenides single crystals. Adv Funct Mater, 2016, 26: 2009–2015
145 Zhang E, Wang P, Li Z, et al. Tunable ambipolar polarization-sensitive photodetectors based on high anisotropy $ReSe_2$. ACS Nano, 2016, 10: 8067–8077
146 Liu B, Chen L, Liu G, et al. High-performance chemical sensing using Schottky-contacted chemical vapor deposition grown monolayer $MoS_2$ transistors. ACS Nano, 2014, 8: 5304–5314
147 Li H, Yin Z, He Q, et al. Layered nanomaterials: Fabrication of single- and multilayer $MoS_2$ film-based field-effect transistors for sensing NO at room temperature. Small, 2012, 8: 63–67
148 Ko K Y, Song J G, Kim Y, et al. Improvement of gas-sensing performance of large-area tungsten disulfide nanosheets by surface functionalization. ACS Nano, 2016, 10: 1–13
149 Wang H, Yu L, Lee Y H, et al. Integrated circuits based on bilayer $MoS_2$ transistors. Nano Lett, 2012, 12: 4674
150 Lin Z, Mccreary A, Briggs N, et al. 2D materials advances: From large scale synthesis and controlled heterostructures to improved characterization techniques, defects and applications. 2D Mater, 2017, 3: 042001
151 Sachid A B, Tosun M, Desai S B, et al. Monolithic 3D CMOS using layered semiconductors. Adv Mater, 2016, 28: 2547–2554
152 Sarkar D, Xie X, Liu W, et al. A subthermionic tunnel field-effect transistor with an atomically thin channel. Nature, 2015, 526: 91–95

Summary for “面向微电子应用的二维过渡金属硫族化合物制备进展”

# Recent progress in two-dimensional transition metal dichalcogenides: Material synthesis for microelectronics

XU Hu, LIAO FuYou, GUO ZhongXun, GUO XiaoJiao, ZHOU Peng, BAO WenZhong* & ZHANG David Wei

*State Key Laboratory of ASIC and System, School of Microelectronics, Fudan University, Shanghai 200433, China*
* Corresponding author, E-mail: baowz@fudan.edu.cn

The size of modern electronic and optoelectronic devices has been shrunk down to nanoscale and this effort still continues. A lot of concerns focus on whether current silicon-based complementary metal oxide semiconductor (CMOS) technologies can overcome the physical limit at nanoscale. A promising alternative choice of semiconductor material, two-dimensional layered materials (2DLMs) have emerged recently, including graphene, 2D transition-metal dichalcogenides (2D TMDs), black phosphors (BPs), etc. Due to their unique atomic thickness nature, 2DLMs are likely to have the greatest potential to overcome the dilemma of geometric scaling. 2DLMs also exhibit a wide range of unique properties owing to their unusual atomically thin defined structures.

Most 2D TMDs have a $MX_2$ structure, where M represents transition metal (Mo, W, Ti, Pt, Hf, etc.) and X is the chalcogen (S, Se, or Te). Contrary to graphene which displays many superior properties but lacks a bandgap, 2D TMDs exhibit a wide range of electronic properties, from semiconducting to metallic or even superconducting, depending on the combination of M and X. For most Mo and W based 2D TMDs, the intrinsic band gap is greater than 1 eV so that the high on/off-current ratio is more easily achieved at room temperature. Moreover, 2D TMDs possess band structures that are known to be highly sensitive to various effects that arise from surfaces and interfaces, thus providing versatile knobs for tuning 2D TMD devices. Various modification methods have been applied to further physically or chemically tune 2DLMs based on their unique intrinsic properties. To date these include dimensional sizing, ion-intercalation, application of an external field, tuning the stacking order, and strain engineering, etc. These fundamental modification methods provide useful engineering tools to improve TMD electronic devices.

So far, most research results of 2D TMDs have been based on mechanically exfoliated sheets which are single crystalline with few defects. But the exfoliation method has poor reproducibility, relatively low yield, and gives rise to a lateral size no more than hundreds of microns. Thus, the main bottleneck for practical application of 2D TMDs in electronic devices still remains at the stage of wafer scale uniform growth. Compared to chemical vapor deposition (CVD) synthesized graphene film with high carrier mobility and large grain size, the existing synthetic methods of 2D TMDs can only produce films with limited spatial uniformity and fair electrical performance. Thus, there is still significant room for improving current CVD methods, or exploring new synthetic methods.

In this review, we summarize and compare various preparation methods of 2D TMD materials. All these methods can be actually classified by two strategies: “Top-down” methods, where the bulk forms are exfoliated into few-layer or monolayer sheets; and the “bottom-up” methods, that chemically synthesize 2D TMDs using CVD, atomic layer deposition (ALD), molecular beam epitaxy (MBE), etc. We first introduce several important “Top-down” methods including mechanical exfoliation, liquid phase exfoliation, ion intercalation and laser thinning. We then focus on the CVD approaches that are suitable for wafer-scale synthesis of high-quality 2D TMD films. We also introduce the latest development of 2D TMDs application in electronic devices, and provide a look at the future of this field.

**two-dimensional layered materials/two-dimensional atomic crystal, transition metal chalcogenide, molybdenum disulfide, chemical vapor deposition**

doi: 10.1360/N972017-00851